

High-Fidelity Control and Entanglement of Rydberg-Atom Qubits

Harry Levine,^{1*} Alexander Keesling,¹ Ahmed Omran,¹ Hannes Bernien,¹ Sylvain Schwartz,² Alexander S. Zibrov,¹ Manuel Endres,³ Markus Greiner,¹ Vladan Vuletić,⁴ and Mikhail D. Lukin¹

¹*Department of Physics, Harvard University, Cambridge, Massachusetts 02138, USA*

²*Laboratoire Kastler Brossel, ENS-PSL Research University, CNRS, Sorbonne Université, Collège de France, 24 rue Lhomond, 75005 Paris, France*

³*Division of Physics, Mathematics and Astronomy, California Institute of Technology, Pasadena, California 91125, USA*

⁴*Department of Physics and Research Laboratory of Electronics, Massachusetts Institute of Technology, Cambridge, Massachusetts 02139, USA*



(Received 12 June 2018; published 20 September 2018)

Individual neutral atoms excited to Rydberg states are a promising platform for quantum simulation and quantum information processing. However, experimental progress to date has been limited by short coherence times and relatively low gate fidelities associated with such Rydberg excitations. We report progress towards high-fidelity quantum control of Rydberg-atom qubits. Enabled by a reduction in laser phase noise, our approach yields a significant improvement in coherence properties of individual qubits. We further show that this high-fidelity control extends to the multi-particle case by preparing a two-atom entangled state with a fidelity exceeding 0.97(3), and extending its lifetime with a two-atom dynamical decoupling protocol. These advances open up new prospects for scalable quantum simulation and quantum computation with neutral atoms.

DOI: [10.1103/PhysRevLett.121.123603](https://doi.org/10.1103/PhysRevLett.121.123603)

Neutral atoms are attractive building blocks for large-scale quantum systems. They can be well isolated from the environment, enabling long-lived quantum memories. Initialization, control, and readout of their internal and motional states is accomplished by resonance methods developed over the past four decades [1]. Recent experiments demonstrated that arrays with a large number of identical atoms can be rapidly assembled while maintaining single-atom optical control [2–4]. These bottom-up approaches are complementary to the methods involving optical lattices loaded with ultracold atoms prepared via evaporative cooling [5], and generally result in atom separations of several micrometers. In order to utilize these arrays for quantum simulation and quantum information processing, it is necessary to introduce controllable interactions between the atoms. This can be achieved by coherent coupling to highly excited Rydberg states, which exhibit strong, long-range interactions [6]. Over the past decade, this approach has emerged as a powerful platform for many applications, including fast multiqubit quantum gates [7–13], quantum simulations of Ising-type spin models with up to 250 spins [14–20], and the study of collective behavior in mesoscopic ensembles [21–25]. Despite these impressive demonstrations, experimental progress to date has been limited by short coherence times and relatively low gate fidelities associated with such Rydberg excitations [8]. This imperfect coherence limits the quality of quantum simulations, and it especially dims the prospects for neutral atom quantum information

processing. The limited coherence becomes apparent even at the level of single isolated atomic qubits [26].

This Letter reports the experimental realization of high-fidelity quantum control of Rydberg-atom qubits. We show that by reducing laser phase noise, a significant improvement in the coherence properties of individual qubits can be achieved, consistent with recent theoretical analysis [26]. We further demonstrate that this high-fidelity control extends to the multiparticle case by preparing a two-atom entangled state with a fidelity exceeding 0.97(3). Finally, we extend the lifetime of the prepared Bell state with a novel two-atom dynamical decoupling protocol.

Our experimental setup has been described in detail previously [3,17]. We deterministically prepare individual cold Rubidium-87 atoms in optical tweezers at programmable positions in one dimension. The atoms are initialized in a Zeeman sublevel $|g\rangle = |5S_{1/2}, F=2, m_F=-2\rangle$ of the ground state via optical pumping in a 1.5 G magnetic field [27]. We then rapidly switch off the tweezer potentials, and apply a laser field to couple the atoms to the Rydberg state $|r\rangle = |70S, J=1/2, m_J=-1/2\rangle$. After the laser pulse of typical duration 3–8 μs , we restore the tweezer potentials. Atoms that are in the ground state are recaptured by the tweezers, whereas those left in the Rydberg state are pushed away by the tweezer beams [26]. This simple detection method has Rydberg state detection fidelity $f_r = 0.96(1)$ and ground state detection fidelity f_g , ranging from 0.955(5) to 0.990(2), depending on the trap-off time [27].

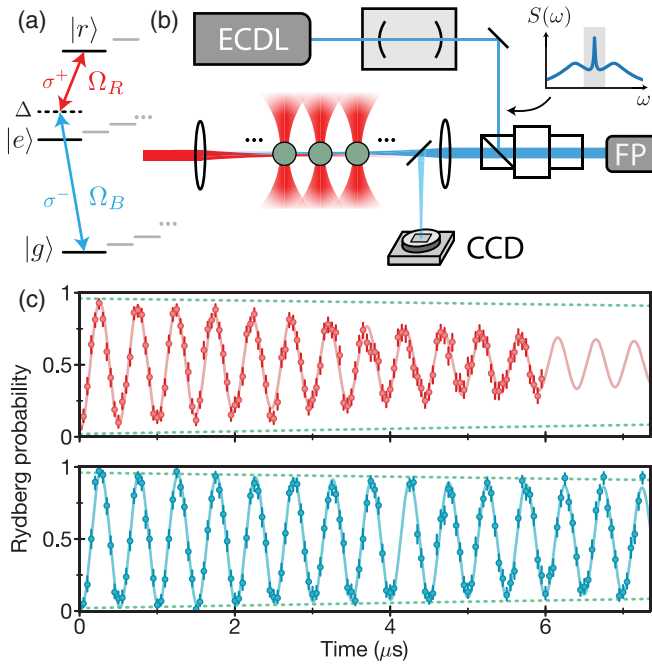


FIG. 1. Experimental setup and single-atom Rabi oscillations. (a) The ground state $|g\rangle = |5S_{1/2}, F = 2, m_F = -2\rangle$ is coupled to $|r\rangle = |70S, J = 1/2, m_J = -1/2\rangle$ via the intermediate state $|e\rangle = |6P_{3/2}, F = 3, m_F = -3\rangle$. (b) The lasers are locked to a reference cavity whose narrow transmission window (shaded region in inset) suppresses high-frequency phase noise. This transmitted light is used to injection lock a Fabry-Perot (FP) laser diode. The laser diode output is focused onto the array of atoms trapped in optical tweezers, with a small pickoff onto a reference CCD camera used for alignment. (c) Resonant two-photon coupling induces Rabi oscillations between $|g\rangle$ and $|r\rangle$. The upper plot is a typical measurement from the previous setup used in [17]. The lower plot shows typical results with the new setup, with a fitted coherence time of $27(4) \mu\text{s}$. Each data point is calculated from 50–100 repeated measurements of two identically coupled atoms separated by $23 \mu\text{m}$ such that they are effectively non-interacting. In all figures, error bars mark 68% confidence intervals, solid lines are fits to experimental data, and dotted lines indicate the expected contrast from the numerical model.

In our experiments, the Rydberg states are excited via a two-photon transition. A 420 nm laser is blue detuned by Δ from the transition from $|g\rangle$ to $|e\rangle = |6P_{3/2}, F = 3, m_F = -3\rangle$. A second laser field at 1013 nm couples $|e\rangle$ to $|r\rangle$. The two lasers are polarized to drive σ^- and σ^+ transitions, respectively, such that only a single intermediate sublevel and Rydberg state can be coupled, avoiding the population of additional levels and associated dephasing [see Fig. 1(a)].

The two lasers (external-cavity diode lasers from MogLabs) are frequency stabilized by a Pound-Drever-Hall (PDH) lock to an ultra-low expansion reference cavity (StableLasers). The PDH lock strongly suppresses laser noise at frequencies below the effective bandwidth of the lock, resulting in narrow linewidths of <1 kHz, as

estimated from in-loop noise. However, noise above the lock bandwidth cannot be suppressed, and can be amplified at high locking gain. This results in broad peaks in phase noise around $\sim 2\pi \times 1$ MHz [see inset of Fig. 1(b)]. This high-frequency phase noise has been reported as a known coherence limitation in Rydberg experiments [26] and experiments with trapped ions [30,31], and has also been studied in the context of atomic clocks [32]. To suppress this phase noise, we follow the approach of [30,31,33,34] in which the reference cavity is used as a spectral filter. In particular, the transmission function of the cavity is a Lorentzian with a full width at half maximum of $\Gamma \sim 2\pi \times 500$ kHz (corresponding to a finesse of $F \sim 3000$). When the laser is locked, its narrow linewidth carrier component is transmitted through the cavity, whereas the power spectral density $2\pi \times 1$ MHz away from the carrier is suppressed by a factor of $\gtrsim 16$ (estimated using the cavity linewidth). To amplify the transmitted light at both 420 and 1013 nm, we split the two colors and use each beam to injection lock a separate laser diode (1013 nm from Toptica, 420 nm from TopGaN), which inherits the same spectral properties. This amplifies the spectrally pure transmitted light to 5 mW of 420 nm and 50 mW of 1013 nm light. While the 420 nm power is sufficient to drive the blue transition directly, the 1013 nm is further amplified by a tapered amplifier (MogLabs).

We focus both lasers onto the atom array in a counter-propagating configuration to minimize Doppler shifts due to finite atomic temperature. The 420 (1013) nm laser is focused to a waist of $20(30) \mu\text{m}$. We achieve single-photon Rabi frequencies of $\Omega_B \simeq 2\pi \times 54$ MHz ($\Omega_R \simeq 2\pi \times 40$ MHz). At our intermediate detuning of $\Delta \simeq 2\pi \times 540$ MHz, this leads to a two-photon Rabi frequency of $\Omega = \Omega_B \Omega_R / (2\Delta) \simeq 2\pi \times 2$ MHz. Each beam is power stabilized to $<1\%$ by an acousto-optic modulator that is also used for fast (~ 20 ns) switching. We use a sample-and-hold method to pause the intensity lock during the Rydberg pulses to avoid introducing additional intensity noise. To minimize sensitivity to pointing fluctuations, we ensure well-centered alignment onto the atoms using a reference camera [depicted in Fig. 1(b)] and an automatic beam alignment procedure [27].

With these technical improvements in place, we measure long-lived Rabi oscillations with a $1/e$ lifetime of $\tau = 27(4) \mu\text{s}$, to be compared with a typical $\lesssim 7 \mu\text{s}$ lifetime in previous experiments [17] [see Fig. 1(c)]. Importantly, we observe excellent agreement between these new measurements and a simple numerical model for our single-atom system, indicated by dotted lines in all figures. The numerical model has no free parameters and accounts only for the effects of random Doppler shifts, off-resonant scattering from the intermediate state, the Rydberg state lifetime, and finite detection fidelity [27]. In the case of resonant Rabi oscillations, the primary limitation is off-resonant scattering.

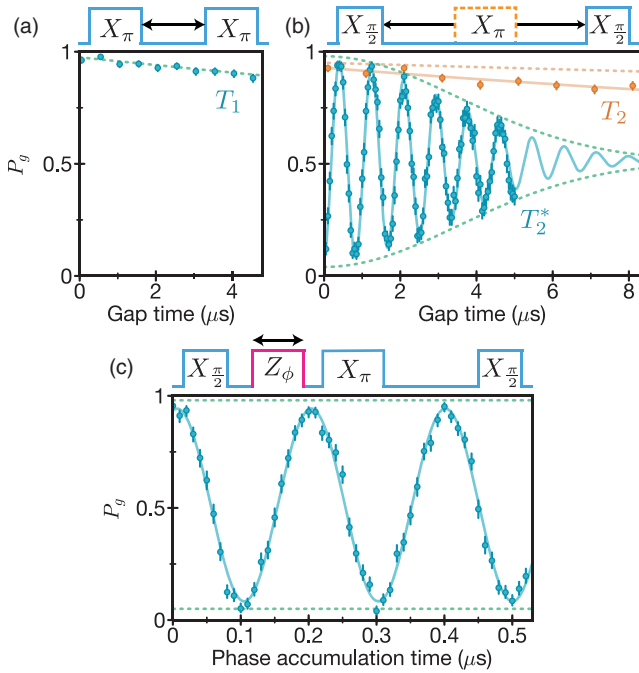


FIG. 2. Characterization of single-atom coherence and phase control. (a) The lifetime of $|r\rangle$ is measured by exciting from $|g\rangle$ to $|r\rangle$ with a π pulse, and then deexciting after a variable delay. The probability to end in $|g\rangle$ (denoted P_g) decays with an extracted lifetime of $T_1 = 51(6) \mu\text{s}$ (fitted to an exponential decay model with no offset). (b) A Ramsey experiment (blue) shows Gaussian decay with a $1/e$ lifetime of $T_2^* = 4.5(1) \mu\text{s}$, limited by thermal Doppler shifts. Inserting an additional π pulse (orange) between the $\pi/2$ pulses cancels the effect of the Doppler shifts and results in a substantially longer coherence lifetime of $T_2 = 32(6) \mu\text{s}$ (fitted to an exponential decay model with an offset of 0.5). (c) A single-atom phase gate is implemented by applying an independent 809 nm laser which induces a light shift $\delta = 2\pi \times 5$ MHz on the ground state for time t , resulting in an accumulated dynamical phase $\phi = \delta t$. The gate is embedded in a spin-echo sequence to cancel Doppler shifts. In each measurement shown here, the 1013 nm laser remains on for the entire pulse sequence, while the 420 nm laser is pulsed according to the sequence shown above each plot. Each data point is calculated from 200–500 repeated measurements with a single atom per realization.

Next, we characterize the coherence of single atoms and demonstrate single-qubit control. To begin, we experimentally measure the lifetime of the Rydberg state in Fig. 2(a). The measured $T_1 = T_{r \rightarrow g} = 51(6) \mu\text{s}$ is consistent with the 146 μs Rydberg state lifetime [35] when combined with the $\sim 80 \mu\text{s}$ timescale for off-resonant scattering of the 1013 nm laser from $|e\rangle$. A Ramsey experiment shows Gaussian decay that is well explained by thermal Doppler shifts [see Fig. 2(b)]. At 10 μK , the random atomic velocity in each shot of the experiment appears as a random detuning δ^D from a Gaussian distribution of width $2\pi \times 43.5$ kHz, resulting in dephasing as $|\psi\rangle \rightarrow (1/\sqrt{2})(|g\rangle + e^{i\delta^D t}|r\rangle)$. However, since the random Doppler shift is constant over the duration of each pulse sequence, its effect can be

eliminated via a spin-echo sequence [orange in Fig. 2(b)]. Note that the spin-echo measurements display some small deviations from the numerical simulations, indicating the presence of an additional dephasing channel. Assuming an exponential decay, we measure a fitted $T_2 = 32(6) \mu\text{s}$ and extract a pure dephasing time $T_\phi = [1/T_2 - 1/(2T_{r \rightarrow g})]^{-1} = 47(13) \mu\text{s}$. We hypothesize that this dephasing may result from residual laser phase noise.

Finally, we demonstrate a single-atom phase gate by applying an independent focused laser that shifts the energy of the ground state $|g\rangle$ [see Fig. 2(c)] [27]. By controlling the duration of the applied laser pulse, we impart a controlled dynamical phase on $|g\rangle$ relative to $|r\rangle$. The contrast of the resulting phase gate (embedded in a spin-echo sequence) is close to the limit imposed by detection and spin-echo fidelity.

We next turn to two-atom control. To this end, we position two atoms at a separation of 5.7 μm , at which the Rydberg-Rydberg interaction is $U/\hbar = 2\pi \times 30$ MHz $\gg \Omega = 2\pi \times 2$ MHz. In this so-called Rydberg blockade regime, the laser field globally couples both atoms from $|gg\rangle$ to the symmetric state $|W\rangle = (1/\sqrt{2})(|gr\rangle + |rg\rangle)$ at an enhanced Rabi frequency of $\sqrt{2}\Omega$ [see Fig. 3(a)] (here the excited states $|r\rangle$ are defined in the rotating frame to incorporate the spatial phase factors e^{ikx} , as discussed in [27]). The measured probabilities for the states $|gg\rangle$, $|gr\rangle$, $|rg\rangle$, and $|rr\rangle$ (denoted by P_{gg} , P_{gr} , P_{rg} , and P_{rr} , respectively) show that indeed no population enters the doubly excited state ($P_{rr} < 0.02$, consistent with only detection error). Instead, there are oscillations between the manifold of zero excitations and the manifold of one excitation with a fitted frequency of $2\pi \times 2.83$ MHz $\approx \sqrt{2}\Omega$ [see Fig. 3(b)].

These collective Rabi oscillations can be used to directly prepare the maximally entangled Bell state $|W\rangle$ by applying a π pulse at the enhanced Rabi frequency (denoted by X_π^W). To determine the fidelity of this experimentally prepared entangled state, given by $\mathcal{F} = \langle W|\rho|W\rangle$, we express it in terms of diagonal and off diagonal matrix elements of the density operator ρ :

$$\mathcal{F} = \frac{1}{2}(\rho_{gr,gr} + \rho_{rg,rg}) + \frac{1}{2}(\rho_{gr,rg} + \rho_{rg,gr}), \quad (1)$$

where $\rho_{\alpha\beta,\gamma\delta} = \langle \alpha\beta|\rho|\gamma\delta\rangle$ for $\alpha, \beta, \gamma, \delta \in \{g, r\}$. The diagonal elements can be directly measured by applying a π pulse and then measuring the populations. The results closely match those of a perfect $|W\rangle$ state after accounting for state detection errors, with $\rho_{gr,gr} + \rho_{rg,rg} = 0.94(1)$, relative to a maximum possible value of 0.95(1).

To measure the off diagonal elements of the density matrix, we make use of the single-atom phase gate $Z_\phi^{(1)}$ demonstrated in Fig. 2(c), which introduces a variable phase on one atom (as demonstrated in [36]). Specifically, a local beam adds a light shift δ to $|gr\rangle$ but not to $|rg\rangle$,

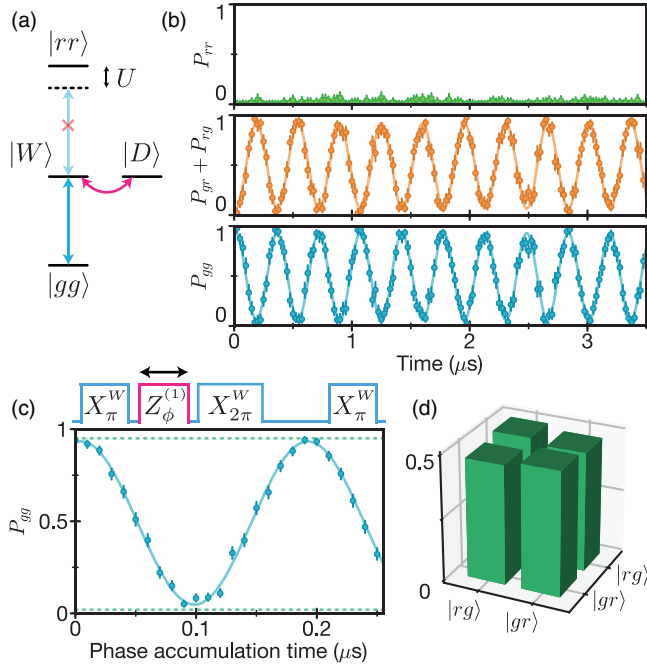


FIG. 3. Coherent control and entanglement generation with two atoms. (a) The level structure for two nearby atoms features a doubly excited state $|rr\rangle$, which is shifted by the interaction energy $U \gg \hbar\Omega$. In this Rydberg blockade regime, the laser field only couples $|gg\rangle$ to $|W\rangle$. The symmetric and antisymmetric states $|W\rangle$, $|D\rangle = (1/\sqrt{2})(|gr\rangle \pm |rg\rangle)$ can be coupled by a local phase gate on one atom (pink arrow). (b) After driving both atoms on resonance for variable time, we measure the probability of the resulting two-atom states. Population oscillates from $|gg\rangle$ to $|W\rangle$ at the enhanced Rabi frequency $\sqrt{2}\Omega$. (c) We measure the entanglement fidelity of the two atoms after a resonant π pulse in the blockade regime. A local phase gate $Z_\phi^{(1)}$ rotates $|W\rangle$ into $|D\rangle$, which is detected by a subsequent π pulse. The fitted contrast 0.88(2) measures the off diagonal density matrix elements. The phase gate is implemented by an off resonant laser focused onto one atom, with a crosstalk of $<2\%$ [27]. The measurement is embedded in a spin-echo sequence to cancel dephasing from thermal Doppler shifts. (d) The four components of the density matrix correspond to an entangled state with fidelity $\mathcal{F} = 0.97(3)$ (corrected for detection error). Each data point in (b) and (c) is calculated from ~ 50 and ~ 250 repeated measurements, respectively, with a single atom pair per realization. Dotted lines in (c) mark the limits of detection fidelity.

such that $|W\rangle \rightarrow (1/\sqrt{2})(e^{i\delta t}|gr\rangle + |rg\rangle)$. This phase accumulation rotates $|W\rangle$ into the orthogonal dark state $|D\rangle = (1/\sqrt{2})(|gr\rangle - |rg\rangle)$ according to the following:

$$|W\rangle \rightarrow \cos(\delta t/2)|W\rangle + i \sin(\delta t/2)|D\rangle. \quad (2)$$

Since $|D\rangle$ is uncoupled by the laser field, a subsequent π pulse maps only the population of $|W\rangle$ back to $|gg\rangle$. The probability of the system to end in $|gg\rangle$ therefore depends on the phase accumulation time as $P_{gg}(t) = A \cos^2(\delta t/2)$.

Here, the amplitude of the oscillation A precisely measures the off diagonal matrix elements $\rho_{gr,rg} = \rho_{rg,gr}$ (see [27] for derivation). Note that in order to mitigate sensitivity to random Doppler shifts, we embed this entire sequence in a spin-echo protocol [see Fig. 3(c)]. The resulting contrast is $A = 0.88(2) = 2\rho_{gr,rg} = 2\rho_{rg,gr}$. Combining these values with the diagonal matrix elements, we have directly measured entanglement fidelity of $\mathcal{F} = 0.91(2)$. The maximum measurable fidelity given our state detection error rates would be 0.94(2), so after correcting for imperfect detection, we find that the entangled Bell state was created with fidelity of $\mathcal{F} = 0.97(3)$. We note that this fidelity includes errors introduced during the pulses that follow the initial π pulse, and therefore constitutes a lower bound on the true fidelity.

Finally, we explore the lifetime of the entangled state by exciting $|W\rangle$ with a π pulse and then deexciting after a variable delay (see Fig. 4). The decay in contrast is in good agreement with numerical predictions associated with random Doppler shifts. In particular, the two components $|gr\rangle$ and $|rg\rangle$ of the $|W\rangle$ state dephase as $|W\rangle \rightarrow (1/\sqrt{2})(e^{i\delta_1^D t}|gr\rangle + e^{i\delta_2^D t}|rg\rangle)$, where δ_i^D is the two-photon Doppler shift on atom i .

We extend the lifetime of the two-atom entangled state with a many-body echo sequence. After the $|W\rangle$ state has evolved for time T , we apply a 2π pulse to the two-atom system. In the Rydberg blockade regime, such a pulse swaps the populations of $|gr\rangle$ and $|rg\rangle$. After again evolving for time T , the total accumulated Doppler shifts are the

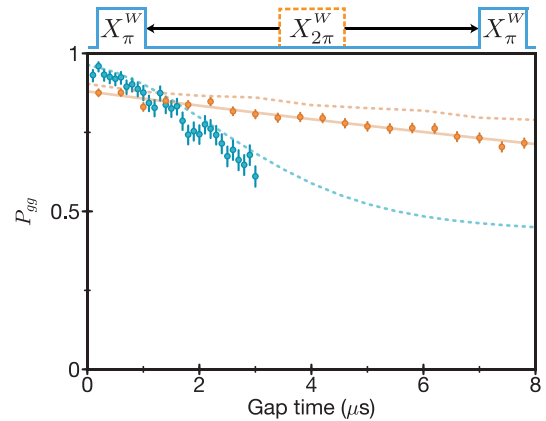


FIG. 4. Extension of entangled-state lifetime via dynamical decoupling. We measure the lifetime of $|W\rangle$ by exciting $|gg\rangle$ to $|W\rangle$ and then deexciting after a variable time (blue). The lifetime is limited by dephasing from random Doppler shifts. Inserting an additional 2π pulse (orange) in the blockade regime swaps the populations of $|gr\rangle$ and $|rg\rangle$ to refocus the random phase accumulation, extending the lifetime to $\sim 36 \mu\text{s}$ (fitted to an exponential decay with no offset, shown as the solid orange line). The initial offset in each curve is set by the ground state detection fidelity associated with the given trap-off time. All data points are calculated from 30–100 repeated measurements, averaged over nine independent, identically coupled atom pairs per realization.

same for each part of the two-atom wave function, and therefore do not affect the final $|W\rangle$ state fidelity. Indeed, Fig. 4 shows that its lifetime is extended far beyond the Doppler-limited decay to $T_2^W = 36(2) \mu\text{s}$. As in the single atom case, we extract a pure dephasing timescale $T_\phi^W = (1/T_2^W - 1/T_{r \rightarrow g})^{-1} > 100 \mu\text{s}$.

Remarkably, the Bell state dephasing time $T_\phi^W > 100 \mu\text{s}$ is significantly longer than the single atom dephasing time $T_\phi = 47(13) \mu\text{s}$. This can be understood by noting that the states $|gr\rangle$ and $|rg\rangle$ form a decoherence-free subspace that is insensitive to global perturbations such as laser phase and intensity fluctuations that couple identically to both atoms [37,38]. In contrast, a single atom in a superposition $|\psi\rangle = (1/\sqrt{2})(|g\rangle + |r\rangle)$ is sensitive to both the laser phase and the laser intensity. These measurements provide further indications that laser noise is not completely eliminated in our experiment.

Our measurements establish Rydberg-atom qubits as a competitive platform for high-fidelity quantum simulation and computation. The techniques demonstrated in this Letter are of immediate importance to ongoing experiments using neutral atom arrays. Furthermore, the demonstrated fidelities can be further improved by increasing laser intensities and operating at larger detunings from the intermediate state, thereby reducing the deleterious effect of off-resonant scattering [27], or by using a direct single-photon transition. In addition, sideband cooling of atoms in tweezers [39,40] can dramatically decrease the magnitude of Doppler shifts, while low-noise laser sources such as Titanium-Sapphire lasers or diode lasers filtered by higher-finesse cavities will further eliminate errors caused by phase noise. Advanced control techniques, such as laser pulse shaping, can also be utilized to reach higher fidelities [41]. Finally, state detection fidelities can be improved by mapping Rydberg states to separate ground state levels, which will additionally enable long-term storage of the prepared entangled states.

We acknowledge A. Browaeys, M. Saffman, G. Biedermann, and their groups for many fruitful discussions during the Institute for Theoretical Atomic, Molecular, and Optical Physics (ITAMP) workshop, which stimulated this study. We also thank J. Ye and T. Lahaye for many useful discussions and suggestions. This work was supported by National Science Foundation (NSF), Center for Ultracold Atoms (CUA), Army Research Office (ARO), Air Force Office of Scientific Research Multidisciplinary Research Program of the University Research Initiative (AFOSR MURI), and the Vannevar Bush Faculty Fellowship. H.L. acknowledges support from the National Defense Science and Engineering Graduate (NDSEG) fellowship. A. O. acknowledges support by a research fellowship from the German Research Foundation (DFG). S. S. acknowledges funding from the European Union under the Marie Skłodowska Curie Individual Fellowship Programme H2020-MSCA-IF-2014 (Project No. 658253).

*hlevine@g.harvard.edu

- [1] D. Weiss and M. Saffman, Quantum computing with neutral atoms, *Phys. Today* **70**, No. 7, 44 (2017).
- [2] D. Barredo, S. de Léséleuc, V. Lienhard, T. Lahaye, and A. Browaeys, An atom-by-atom assembler of defect-free arbitrary two-dimensional atomic arrays, *Science* **354**, 1021 (2016).
- [3] M. Endres, H. Bernien, A. Keesling, H. Levine, E. R. Anschuetz, A. Krajenbrink, C. Senko, V. Vuletić, M. Greiner, and M. D. Lukin, Atom-by-atom assembly of defect-free one-dimensional cold atom arrays, *Science* **354**, 1024 (2016).
- [4] H. Kim, W. Lee, H. Lee, H. Jo, Y. Song, and J. Ahn, *In situ* single-atom array synthesis using dynamic holographic optical tweezers, *Nat. Commun.* **7**, 13317 (2016).
- [5] C. Gross and I. Bloch, Quantum simulations with ultracold atoms in optical lattices, *Science* **357**, 995 (2017).
- [6] A. Browaeys, D. Barredo, and T. Lahaye, Experimental investigations of dipole-dipole interactions between a few Rydberg atoms, *J. Phys. B* **49**, 152001 (2016).
- [7] D. Jaksch, J. I. Cirac, P. Zoller, S. L. Rolston, R. Côté, and M. D. Lukin, Fast Quantum Gates for Neutral Atoms, *Phys. Rev. Lett.* **85**, 2208 (2000).
- [8] M. Saffman, Quantum computing with atomic qubits and Rydberg interactions: progress and challenges, *J. Phys. B* **49**, 202001 (2016).
- [9] T. Wilk, A. Gaëtan, C. Evellin, J. Wolters, Y. Miroshnychenko, P. Grangier, and A. Browaeys, Entanglement of Two Individual Neutral Atoms Using Rydberg Blockade, *Phys. Rev. Lett.* **104**, 010502 (2010).
- [10] L. Isenhower, E. Urban, X. L. Zhang, A. T. Gill, T. Henage, T. A. Johnson, T. G. Walker, and M. Saffman, Demonstration of a Neutral Atom Controlled-NOT Quantum Gate, *Phys. Rev. Lett.* **104**, 010503 (2010).
- [11] K. M. Maller, M. T. Lichtman, T. Xia, Y. Sun, M. J. Piotrowicz, A. W. Carr, L. Isenhower, and M. Saffman, Rydberg-blockade controlled-NOT gate and entanglement in a two-dimensional array of neutral-atom qubits, *Phys. Rev. A* **92**, 022336 (2015).
- [12] Y.-Y. Jau, A. M. Hankin, T. Keating, I. H. Deutsch, and G. W. Biedermann, Entangling atomic spins with a Rydberg-dressed spin-flip blockade, *Nat. Phys.* **12**, 71 (2016).
- [13] Y. Zeng, P. Xu, X. He, Y. Liu, M. Liu, J. Wang, D. J. Papoular, G. V. Shlyapnikov, and M. Zhan, Entangling Two Individual Atoms of Different Isotopes via Rydberg Blockade, *Phys. Rev. Lett.* **119**, 160502 (2017).
- [14] P. Schauß, J. Zeiher, T. Fukuhara, S. Hild, M. Cheneau, T. Macrì, T. Pohl, I. Bloch, and C. Gross, Crystallization in Ising quantum magnets, *Science* **347**, 1455 (2015).
- [15] H. Labuhn, D. Barredo, S. Ravets, S. de Léséleuc, T. Macrì, T. Lahaye, and A. Browaeys, Tunable two-dimensional arrays of single Rydberg atoms for realizing quantum Ising models, *Nature (London)* **534**, 667 (2016).
- [16] J. Zeiher, R. van Bijnen, P. Schauß, S. Hild, J. Choi, T. Pohl, I. Bloch, and C. Gross, Many-body interferometry of a Rydberg-dressed spin lattice, *Nat. Phys.* **12**, 1095 (2016).
- [17] H. Bernien, S. Schwartz, A. Keesling, H. Levine, A. Omran, H. Pichler, S. Choi, A. S. Zibrov, M. Endres, M. Greiner, V. Vuletić, and M. D. Lukin, Probing many-body dynamics on

- a 51-atom quantum simulator, *Nature (London)* **551**, 579 (2017).
- [18] V. Lienhard, S. de Léséleuc, D. Barredo, T. Lahaye, A. Browaeys, M. Schuler, L.-P. Henry, and A. M. Läuchli, Observing the Space- and Time-Dependent Growth of Correlations in Dynamically Tuned Synthetic Ising Models with Antiferromagnetic Interactions, *Phys. Rev. X* **8**, 021070 (2018).
- [19] E. Guardado-Sanchez, P. T. Brown, D. Mitra, T. Devakul, D. Huse, P. Schauß, and W. S. Bakr, Probing the Quench Dynamics of Antiferromagnetic Correlations in a 2D Quantum Ising Spin System, *Phys. Rev. X* **8**, 021069 (2018).
- [20] H. Kim, Y. J. Park, K. Kim, H.-S. Sim, and J. Ahn, Detailed Balance of Thermalization Dynamics in Rydberg-Atom Quantum Simulators, *Phys. Rev. Lett.* **120**, 180502 (2018).
- [21] K. Singer, M. Reetz-Lamour, T. Amthor, L. G. Marcassa, and M. Weidemüller, Suppression of Excitation and Spectral Broadening Induced by Interactions in a Cold Gas of Rydberg Atoms, *Phys. Rev. Lett.* **93**, 163001 (2004).
- [22] R. Heidemann, U. Raitzsch, V. Bendkowsky, B. Butscher, R. Löw, L. Santos, and T. Pfau, Evidence for Coherent Collective Rydberg Excitation in the Strong Blockade Regime, *Phys. Rev. Lett.* **99**, 163601 (2007).
- [23] Y. O. Dudin, L. Li, F. Bariani, and A. Kuzmich, Observation of coherent many-body Rabi oscillations, *Nat. Phys.* **8**, 790 (2012).
- [24] T. M. Weber, M. Hönig, T. Niederprüm, T. Manthey, O. Thomas, V. Guarrera, M. Fleischhauer, G. Barontini, and H. Ott, Mesoscopic Rydberg-blockaded ensembles in the superatom regime and beyond, *Nat. Phys.* **11**, 157 (2015).
- [25] O. Firstenberg, C. S. Adams, and S. Hofferberth, Nonlinear quantum optics mediated by Rydberg interactions, *J. Phys. B* **49**, 152003 (2016).
- [26] S. de Léséleuc, D. Barredo, V. Lienhard, A. Browaeys, and T. Lahaye, Analysis of imperfections in the coherent optical excitation of single atoms to Rydberg states, *Phys. Rev. A* **97**, 053803 (2018).
- [27] See Supplemental Material at <http://link.aps.org/supplemental/10.1103/PhysRevLett.121.123603>, which includes Refs. [28,29].
- [28] J. R. Johansson, P. D. Nation, and F. Nori, QuTiP 2: A Python framework for the dynamics of open quantum systems, *Comput. Phys. Commun.* **184**, 1234 (2013).
- [29] D. D. Yavuz, P. B. Kulatunga, E. Urban, T. A. Johnson, N. Proite, T. Henage, T. G. Walker, and M. Saffman, Fast Ground State Manipulation of Neutral Atoms in Microscopic Optical Traps, *Phys. Rev. Lett.* **96**, 063001 (2006).
- [30] N. Akerman, N. Navon, S. Kotler, Y. Glickman, and R. Ozeri, Universal gate-set for trapped-ion qubits using a narrow linewidth diode laser, *New J. Phys.* **17**, 113060 (2015).
- [31] L. Gerster, Spectral filtering and laser diode injection for multi-qubit trapped ion gates, Master Thesis, ETH Zurich, 2015.
- [32] M. Martin, Quantum metrology and many-body physics: Pushing the frontier of the optical lattice clock, Ph.D. Thesis, JILA, 2013.
- [33] J. Hald and V. Ruseva, Efficient suppression of diode-laser phase noise by optical filtering, *J. Opt. Soc. Am. B* **22**, 2338 (2005).
- [34] T. Nazarova, C. Lisdat, F. Riehle, and U. Sterr, Low-frequency-noise diode laser for atom interferometry, *J. Opt. Soc. Am. B* **25**, 1632 (2008).
- [35] I. I. Beterov, I. I. Ryabtsev, D. B. Tretyakov, and V. M. Entin, Quasiclassical calculations of blackbody-radiation-induced depopulation rates and effective lifetimes of Rydberg nS , nP , and nD alkali-metal atoms with $n \leq 80$, *Phys. Rev. A* **79**, 052504 (2009).
- [36] H. Labuhn, S. Ravets, D. Barredo, L. Béguin, F. Nogrette, T. Lahaye, and A. Browaeys, Single-atom addressing in microtraps for quantum-state engineering using Rydberg atoms, *Phys. Rev. A* **90**, 023415 (2014).
- [37] D. Kielpinski, V. Meyer, M. A. Rowe, C. A. Sackett, W. M. Itano, C. Monroe, and D. J. Wineland, A Decoherence-Free Quantum Memory Using Trapped Ions, *Science* **291**, 1013 (2001).
- [38] C. F. Roos, G. P. T. Lancaster, M. Riebe, H. Häffner, W. Hänsel, S. Gulde, C. Becher, J. Eschner, F. Schmidt-Kaler, and R. Blatt, Bell States of Atoms with Ultralong Lifetimes and Their Tomographic State Analysis, *Phys. Rev. Lett.* **92**, 220402 (2004).
- [39] A. M. Kaufman, B. J. Lester, and C. A. Regal, Cooling a Single Atom in an Optical Tweezer to Its Quantum Ground State, *Phys. Rev. X* **2**, 041014 (2012).
- [40] J. D. Thompson, T. G. Tiecke, A. S. Zibrov, V. Vuletić, and M. D. Lukin, Coherence and Raman Sideband Cooling of a Single Atom in an Optical Tweezer, *Phys. Rev. Lett.* **110**, 133001 (2013).
- [41] L. S. Theis, F. Motzoi, F. K. Wilhelm, and M. Saffman, High-fidelity Rydberg-blockade entangling gate using shaped, analytic pulses, *Phys. Rev. A* **94**, 032306 (2016).